Chapter 8 : Transcranial Doppler Monitoring of the Middle Cerebral Artery

In this chapter, we discuss transcranial Doppler ultrasound (TCD), and how it provides additional insight into the neurophysiology of patients prior to carotid endarterectomy. First, a review is provied of the application of TCD in a clinical monitoring and research setting. Next, techniques to increase the reliability of data collected are covered. Finally, microemboli and peak velocity data collected as part of this study are presented.

8.1   Physiological insights from transcranial Doppler

TCD is a useful tool in research and clinical situations where monitoring of intracranial blood flow is desired. For example, TCD is used in psychology experiments [1], for evaluating the potential for sickle cell stroke [2], estimation of intracranial pressure [3], and inpatient monitoring [4, 3]. TCD is amenable to bedside monitoring or in surgery, is cost-effective, has very good temporal resolution, can collect data for extended time periods, and is non-invasive. However, there are limitations associated with its use. For 10% to 30% of patients, the acoustic window in the skull is too thick to obtain adequate signals, it is sensitive to motion, and it can be difficult to locate vessels with the single element transducer. Collection and analysis of TCD data is also labor intensive and time consuming [5, 3].

The purpose of TCD in this study is to detect microemboli originating from vulnerable carotid plaque. A microemboli passing through the middle cerebral artery (MCA) will result in

what is termed a microembolic ultrasonic signals (MES) or high intensity transient signals (HITS). TCD provides a non-invasive *in vivo* validation of the vulnerability assessment of plaque tissue obtained with strain imaging. Microemboli detected with TCD have been connected to peri-operative symptoms of ipsilateral cerebral ischemia [6, 7].

Furthermore, MES predict future ischemic events such as episodic stroke, transient ischemic attack (TIA) or migraines [8, 9, 10, 11]. In a typical single one hour session, 43% of symptomatic cases and 10% of asymptomatic cases will show one or more MES [8]. If a MES is seen with an asymptomatic case, the risk of stroke or TIA in the future increases significantly [12, 8]. In addition, recent evidence reinforces the supposition that microemboli cause Alzheimer's disease and vascular cognitive dementias or impairment [13, 14, 15].

Microemboli may originate from locations other than the carotid, such as a patent foramen ovale (PFO), other types of right to left shunts other than a PFO, mechanical heart valves, atrial fibrillation, or congestive heart disease. However, for elderly patients, the most common source is thought to be carotid plaques. Unlike emboli of cardiac origin, microemboli from the carotid should be unilateral and ipsilateral to the vulnerable carotid.

TCD requires ultrasonic transmission through the cranium. This can be achieved via four acoustic windows, the transorbital, suboccipital, transtemporal, or retromandibular [3]. Interrogation of the middle cerebral artery is achieved through the transtemporal window directly above the ear where there is thinning of the cranial plate. The MCA is by far the most common vessel examined when searching for microemboli. It is one of the main branches extending from the Circle of Willis, and flow from the internal carotid artery is directed at the MCA. It is necessary to monitor for microemboli at the MCA, a location distal to the plaque, because it would be difficult to monitor all of the plaque and detect dislodging of the microemboli. Clinical

ultrasound currently generates 2D planar images and the resolution is insufficient to detect a microemboli *in vivo*.

Patients are typically monitored for an hour, with one or more microembolic events considered significant [8]. The identification criteria for MES are transient signals, lasting less than 300 milliseconds, at least 3dB higher than the background blood flow signal, unidirectional in velocity, and accompanied by an audible 'snap', 'chirp', or 'moan' [16].

A similar study was performed by Zuromskis et al. [10] where the relationship between MES and traditional ultrasonic vulnerability metrics, echogenicity and blood flow velocities, was examined. The conclusion of that study was as follows: Despite optimum standard anti-platelet therapy, cerebral micro-embolization occurs in 30% of patients with symptomatic carotid artery disease, which might therefore be a possible risk factor for recurrent neurological symptoms. However, the presence of MES is independent of intrastenotic blood flow disturbances and grey scale ultrasound plaque characteristics. The conclusion of that study is that the presence of MES as an indicator of unstable plaque and thereby a possible risk factor for stroke should be evaluated prospectively using various algorithms for plaque classifications [10].

8.2 Methods to increase the robustness of unstable data

8.2.1 Examination room protocol

TCD was performed thus far on a 19 patients using a Multidop-L2 2.54g system made by DWL (Germany). One hour of data is collected immediately following acquisition of the carotid ultrasound data for strain imaging. A pair of 2 MHz transducers are focused on the right and left MCA at the transtemporal acoustic windows and secured with the Marc600 Transcranial Fixation System head unit. The Doppler gate is placed at a depth of 30 to 67 mm depending on

the size of the patient.

TCD is notorious for difficulties when attempting to obtain useable, reliable data. While valuable physiological data can certainly be acquired, consistent collection of this data is a challenge. McMahon et al. examined the reproducibility of TCD acquisition of MCA velocities [17]. Intraobserver variability was high, and interobserver variability was even higher. On the whole, and Bland-Altman analysis resulted in a 95% limit of agreement of ±36.7 cm/s [17]. The experience of ultrasonographer can be critically important, and in that study inter-observer variance between experienced practitioners was ±22.1 cm/s. Other factors that can compromise success include environmental factors and patient compliance [17].

During acquisition there are multiple false-positive HITS detected due to motion or other sources. To address false positives, marks are added to the data indicating a possible true micro-embolic signal or a known motion artifact. This adds important contextual information for retrospective analysis that is otherwise lost. Artifacts can result from the operator making adjustments to the transducer position, which is the most common source of movement artifacts. There are also many types of motion artifacts that come from the patient: head movement, teeth clenching, or snoring, for example. Secure, stable positioning of the head unit is one of the most critical factors for consistent velocity waveform acquisition, and failure of the head unit will cause artifacts or loss of signal. For this device, a velocity spike occurs when changing the gate depth. When surveying an hour's course of velocity data, knowledge of these conditions are important to correctly interpret the data, and a marking system archives these environmental events.
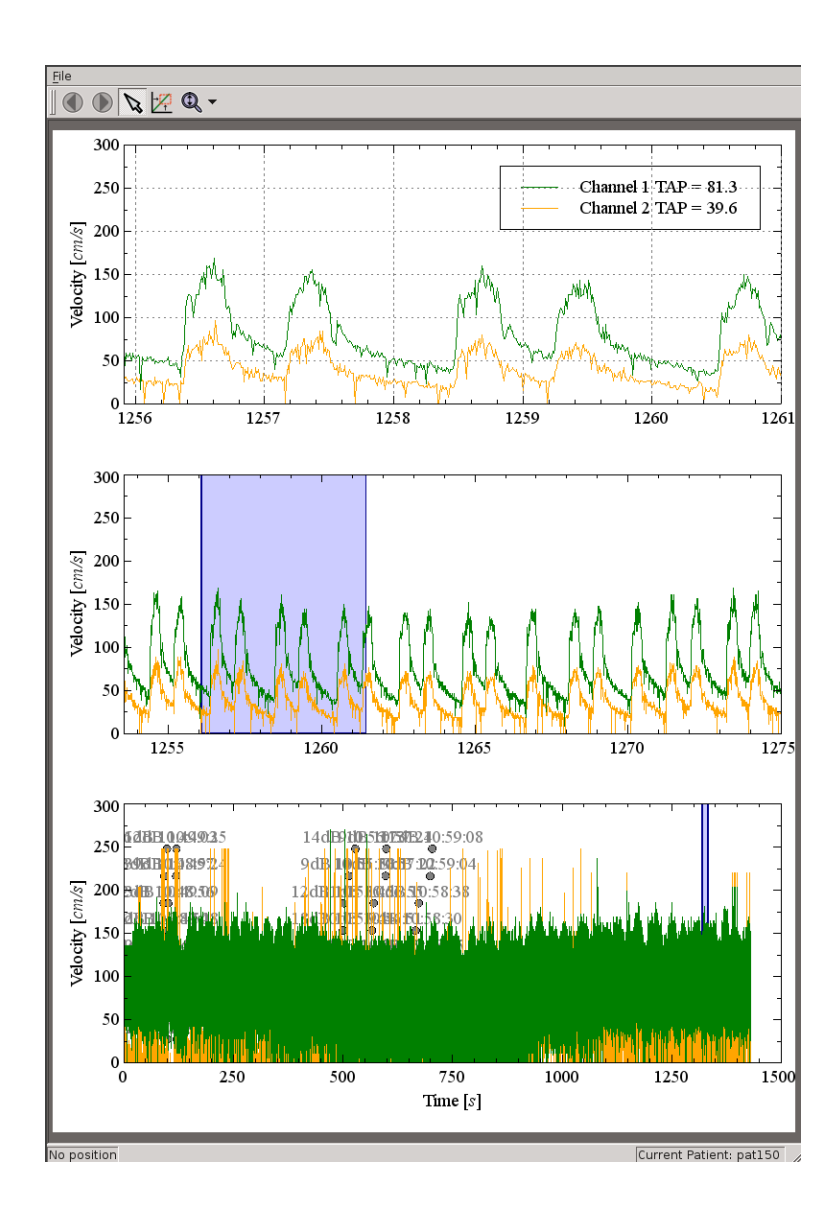
An important practical component of successful data acquisition is patient compliance. Voluntary patient participation is more difficult to attain in the context of anxiety over recent

ischemic events or upcoming surgery. The battery of other tests clinically required to diagnose their condition can lead to test fatigue. Subjects generally find motivation when they become informed of the research purpose of the study during the informed consent process. Retaining subject participation and compliance requires attention to the subject's needs. While pressure the skull from the head unit is unavoidable, patient comfort to the rest of their body helps during the hour long acquisition. A reclined, padded bed with a pillow allows ideal positioning for both the patient and ultrasonographer. While reclined in a flat position for an extended period, a cushion beneath the patient's knees improves back discomfort. Real and perceived burden to the subject are reduced by attention to the environment and time. Professional candor and dress impart patient confidence. Comfort is also assured by scanning in a private room in the clinic or at a facility adjacent to it. Presentation of the scanning room also makes an impression, so efforts are made to ensure cleanliness and removal or concealment of coarse research apparatus that may appear threatening or unsafe. Efforts are made to reduce the time spent for the entire examination; non-critical aspects of the examination are removed, and the entire procedure protocol is defined beforehand. Boredom is a problem as the only task at hand is absence of movement. Reduced lighting in the room helps many subjects to fall asleep, although snoring adds artifacts to the TCD signal.

8.2.2 Retrospective inspection

The Multidop-L2 system displays the power spectrum calculated with a 128 FFT with 67% overlap and a sampling frequency of 1 kHz. The pulse repetition frequency (PRF) is 3 kHz. Additionally, the envelope of the peak velocity for both channels is displayed along with a histogram of High Intensity Transient Signal (HITS). A HITS is recorded whenever the signal exceeds 3 dB over the background signal.

Figure 8.1: TCD post-processing software viewing subject 150. A hierarchical view of the peak velocity data is shown with the shortest time scale on the top plot. Contextual marks made during acquisition, some of which can be seen in the lower plot, are displayed as a dot with the machine recorded time. In this dataset, unilateral elevated peak velocities as well as arrhythmia can be observed.

Post-processing is performed to provide further scrutiny to the collected data. A custom

application was developed to visualize and analyze the available data show in Fig. 8.1.

Interrogating the file system with the native DOS operating system or the BG-Rescue Linux [18]

floppy disk distribution, the files were found to be saved at the *D:\DATA* location. For every

session, sets of files are saved with the *NLA* prefix followed by unique integer incremented for every session. The filename extension has the pattern *T*, followed by a letter indicating the file type, followed by a number starting from zero. This number is incremented every time recording is stopped or started during a session. Two filetypes were found to be of interest: *TX?* and *TW?* where *?* is the acquisition number per session. The *TX?* files are plain text files that contain system setting information and events. Figure 8.2 presents some example content from a *TX?* file. This file first starts with some parameters related to the acquisition such as the patient name and machine settings such as the PRF in Hz, velocity curve sampling frequency in Hz, and the Doppler frequency. Also contained in the *TW?* are HITS are operator mark events, one per line. A HITS event consists of the time the event occurred, in hundredths of seconds after the start of acquisition, the string 'HIT', the amplitude of the HITS in dB, the system clock time, and other numbers. These are algorithmically detected HITS, many of which may be artifacts. A mark event consists of the time the event occurred, in hundredths of seconds after the start of acquisition, the mark number, and the system clock time. Velocity envelope data was found in the *TW?* binary file. This file alternates between left and right channels in 64 sample segments. Each velocity sample is a two byte signed integer. With a sampling rate of 100 Hz, and two bytes per sample, a one hour sessions contains *1,440,000*. This allows the data to be exported on a single 3.5" floppy disk, which has a capacity of 1,474,560 bytes per disk, for further examination. If the file size exceeds disk capacity, the Unix *split* and *cat* programs can be used to transfer the dataset in pieces.

```
"
     0 TEXT FILE VERSION 8.27L
     0 PATIENT  NAME: pat160
     0 PATIENT  EXAM: 08-05-02
     0 SYS PRF 5000
     0 SYS SAMPLE_F 1000
```

```
    0 SYS DOPCHAN 136
    0 SYS EXTCHAN 0
    0 SYS FDOP1 2000
    0 SYS FDOP2 2000
    0 SYS NSAMPLE 2
    0 START  1:41:05
 2728 MRK1  1:41:32   2 MARK1
 5497 TIME  1:42:00
 9213 MRK1  1:42:40   2 MARK1
21500 HIT 11dB  1:44:43   4000T1D050 dS05 X236 dX039 V008    288
21740 MRK1  1:44:45   2 MARK1
22979 MRK1  1:44:58   2 MARK1
23223 TIME  1:45:00
44972 HIT  9dB  1:48:38   4000T1D050 dS05 X184 dX011 V014   1390
...
85464 STOP  1:55:30
```

Figure 8.2: Example content of Multidop-L2 *TX?* file.

A graphical user interface (GUI) was built to retrospectively inspect the recorded data using PyQt4 [19] and Veusz [20]. To expedite analysis of the data collected over an hour time period, three plots of the peak velocity waveform are displayed at three time scales, i.e. the entire acquisition, a 100 second window, and a 5 second window. Clicking on a time segment in the entire acquisition will display the indicated segment in the 100 second window, and clicking on a time segment in the 100 second will display the shaded region in the five second window. Time points where the Multidop-L2 detected a HITS signal are displayed as a non-overlapping dot along with text indicating the magnitude in dB. False and True marks are also displayed as non-overlapping dots, but in distinguishing colors.

8.3 Microemboli and peak velocity results

Microemboli HITS results for subjects where there is reasonable confidence in the reliability of the counts are enumerated in Table 8.1. These results are for up to one hour monitoring prior to surgery. Subject 142 and 143 were monitored both before and after carotid endarterectomy (CEA). Four HITS were noted for Subject 142 prior to surgery and no HITS were detected after

surgery. Subject 143 had no HITS detected before or after CEA. Only guarded confidence is

placed in a subset of the data collected because of factors that prevented the collection of

consitent, reliable signal. Secure positioning of the transducers by the head unit proved to be of

critical importance. Alignment of the acoustic beam with MCA flow is very sensitive to both the

position along the acoustic window and orientation of the transducer. If the head unit cannot

securely anchor the transducer with the skull, constant transducer re-adjustment is required,

which results in poor signal and motion artifacts. The age of the machine also bring into

question reliability of the electronics.

Subject Number	HITS
142	4
143	0
146	1
147	8
148	0
149	1
150	0
151	0
161	0
162	1

Table 8.1: TCD detected microemboli HITS per subject. Only subjects with
reasonable confidence in the results are enumerated.

Subject Number	Side	TAP [cm/s]	Peak Systolic Velocity [cm/s]	Peak Diastolic Velocity [cm/s]	Signal Quality
140	Left	11.3	22.6	6.7	Fair
140	Right	1.8	NS	NS	Poor
142	Left	42.3	71.0	30.3	Good
142	Right	56.7	101.0	37.2	Good
142(post-CEA)	Left	27.0	55.3	19.5	Good
142(post-CEA)	Right	23.9	43.4	17.2	Good
143	Left	11.6	17.7	9.6	Fair
143	Right	NS	NS	NS	Poor
143(post-CEA)	Left	11.2	30.9	5.3	Fair
143(post-CEA)	Right	19	42.8	8.2	Fair
145	Left	8.0	16.1	3.4	Fair
145	Right	8.8	36.7	8.9	Fair
146	Left	3.7	21.4	3.2	Fair
146	Right	7.4	25.5	3.5	Fair
147	Left	8.9	17.9	3.2	Good
147	Right	31.9	61.4	18.7	Good
148	Left	11.1	18.7	8.3	Good
148	Right	3.7	16.0	NS	Fair

149	Left	NS	NS	NS	Poor
149	Right	21.3	29.9	15.1	Good
150	Left	87.5	153.8	60.6	Good
150	Right	40.5	74.3	27.7	Good
151	Left	16.4	32.6	9.9	Fair
151	Right	13.7	NS	NS	Poor
153	Left	48.7	77.7	33.4	Good
153	Right	19.9	37.9	9.6	Fair
154	Left	46.4	84.3	33.6	Good
154	Right	31.4	47.2	23.8	Good
156	Left	12.7	21.6	8.31	Good
156	Right	15.5	26.1	11.0	Good
157	Left	39.0	67.2	29.2	Good
157	Right	47.1	62.7	36.5	Good
158	Left	17.3	26.4	12.0	Good
158	Right	24.4	38.3	19.2	Good
159	Left	36.7	56.6	25.4	Good
159	Right	51.3	81.7	34.5	Good
160	Left	19.5	45.63	10.1	Good
160	Right	21.9	47.04	8.2	Good

161	Left	97.5	182.5	48.1	Good
161	Right	115.1	212.8	55.7	Good
162	Left	22.0	47.52	13.4	Good
162	Right	23.0	48.46	9.6	Good

Table 8.2: Peak velocities as assessed with the analysis software, Fig. 8.1. Measurements are given bilaterally for each side of the subject. The peak velocities in cm/s are shown along with the quality of the signal. No usable signal is indicated with *NS*.

Velocity envelope results are recorded in Table 8.2. Peak systolic velocity (PSV), peak diastolic velocity (PDV), and the time-average-peak (TAP) are shown. There is a large amount of variation across subjects. Some this variation can be attributed to natural variations due to demographics. Velocities in females are relatively higher than males, and velocity on the left side is slightly higher than the right side [21]. Variation may also be due to atherosclerotic effects on hemodynamics. Changes in the TCD measured MCA PSV were correlated with MCA stenosis in a study that validated its findings with magnetic resonance angiography [22]. In cases of focal MCA stenosis, PSV of 140 m/s or higher correlate with a 50% or higher level of stenosis [22]. When there is diffuse stenosis of 50% or higher, PSV exceeded 140 m/s in roughly a quarter of the subjects, but in 54% of the subjects the peak systolic velocity was less than 50 cm/s [22]. Note that two subjects, 150 and 161, exhibited very high unilateral velocities. Right MCA pulsatility index, (PSV - EDV)/MV, where MV is the mean velocity, has been found to have a positive correlation with a global cognitive function test in patients with congestive heart failure [23]. Finally, some velocities may be artificially low because of errors in assumptions about the Doppler angle. The Doppler frequency shift, f_d is given by [24],

$$f_d = \frac{2 f_t V \cos \theta}{c}$$

Eqn. 8.1

It is a function of the transmit frequency, f_t, the blood velocity, V, the speed of sound in tissue, c, and the angle between the axis of the beam and the direction of flow, θ. During TCD, this Doppler angle is assumed to be zero, i.e. the transducer axis is assumed to be parallel to the MCA at the pulse gate. This contrasts to imaging with an array transducer where the B-Mode image can be used to estimate this angle. Although the MCA may be close to being parallel, it is not necessarily the case. The MCA can be tortuous, and its orientation relative acoustic window varies over its course along the lateral sulcus. Position and orientation of the transducer is not dictated solely by the maximum velocity obtained. Good signal can only be attained by positioning the transducer where there is adequate acoustic window, and orientating it so the beam intersects a sufficient blood volume.

8.4 References

[1] F. A. Sorond, D. M. Schnyer, J. M. Serrador, W. P. Milberg and L. A. Lipsitz. Cerebral blood flow regulation during cognitive tasks: effects of healthy aging. *Cortex* 44, 179--184. 2008.

[2] H. A. de Melo, J. A. S. Barreto-Filho, R. C. P. do Prado and R. Cipolotti. Transcranial doppler in sickle cell anaemia: evaluation of brain blood flow parameters in children of Aracaju, Northeast-Brazil. *Arq Neuropsiquiatr* 66, 360--364. 2008.

[3] F. A. Rasulo, E. D. Peri and A. Lavinio. Transcranial Doppler ultrasonography in intensive care. *Eur J Anaesthesiol Suppl* 42, 167--173. 2008.

[4] R. C. McDermid, L. Saxinger, B. Lee, J. Johnstone, R. T. N. Gibney, M. Johnson and S. M. Bagshaw. Human rabies encephalitis following bat exposure: failure of therapeutic coma. *CMAJ* 178, 557--561. 2008.

[5] R. M. Kwee, R. J. van Oostenbrugge, L. Hofstra, G. J. Teule, J. M. A. van Engelshoven, W. H. Mess and M. E. Kooi. Identifying vulnerable carotid plaques by noninvasive imaging. *Neurology* 70, 2401--2409. 2008.

[6] C. R. Levi, H. M. O'Malley, G. Fell, A. K. Roberts, M. C. Hoare, J. P. Royle, A. Chan, B. C. Beiles, B. R. Chambers, C. F. Bladin and G. A. Donnan. Transcranial Doppler detected cerebral microembolism following carotid endarterectomy. High microembolic signal loads predict postoperative cerebral ischaemia. *Brain* 120 (Pt 4, 621--629. 1997.

[7] M. P. Spencer. Transcranial Doppler monitoring and causes of stroke from carotid endarterectomy. *Stroke* 28, 685--691. 1997.

[8] M. A. Ritter, R. Dittrich, N. Thoenissen, E. B. Ringelstein and D. G. Nabavi. Prevalence and prognostic impact of microembolic signals in arterial sources of embolism : A systematic review of the literature. *J Neurol* 255, 953--961. 2008.

[9] J. T. Jesurum, C. J. Fuller, C. J. Kim, K. A. Krabill, M. P. Spencer, J. V. Olsen, W. H. Likosky and M. Reisman. Frequency of migraine headache relief following patent foramen ovale "closure" despite residual right-to-left shunt. *Am J Cardiol* 102, 916--920. 2008.

[10] T. Zuromskis, R. Wetterholm, J. F. Lindqvist, S. Svedlund, C. Sixt, D. Jatuzis, D. Obelieniene, K. Caidahl and R. Volkmann. Prevalence of micro-emboli in symptomatic high grade carotid artery disease: a transcranial Doppler study. *Eur J Vasc Endovasc Surg* 35, 534--540. 2008.

[11] M. Siebler, A. Nachtmann, M. Sitzer, G. Rose, A. Kleinschmidt, J. Rademacher and H. Steinmetz. Cerebral microembolism and the risk of ischemia in asymptomatic high-grade internal carotid artery stenosis. *Stroke* 26, 2184--2186. 1995.

[12] H. S. Markus, D. W. Droste, M. Kaps, V. Larrue, K. R. Lees, M. Siebler and E. B. Ringelstein. Dual antiplatelet therapy with clopidogrel and aspirin in symptomatic carotid stenosis evaluated using doppler embolic signal detection: the Clopidogrel and Aspirin for Reduction of Emboli in Symptomatic Carotid Stenosis (CARESS) trial. *Circulation* 111, 2233--2240. 2005.

[13] N. Purandare, A. Burns, K. J. Daly, J. Hardicre, J. Morris, G. Macfarlane and C. McCollum. Cerebral emboli as a potential cause of Alzheimer's disease and vascular dementia: case-control study. *BMJ* 332, 1119--1124. 2006.

[14] N. Purandare, R. C. O. Voshaar, J. Hardicre, J. Byrne, C. McCollum and A. Burns. Cerebral emboli and depressive symptoms in dementia. *Br J Psychiatry* 189, 260--263. 2006.

[15] N. Purandare, R. C. O. Voshaar, J. Morris, J. E. Byrne, J. Wren, R. F. Heller, C. N. McCollum and A. Burns. Asymptomatic spontaneous cerebral emboli predict cognitive and functional decline in dementia. *Biol Psychiatry* 62, 339--344. 2007.

[16] Anonymous. Basic identification criteria of Doppler microembolic signals. Consensus Committee of the Ninth International Cerebral Hemodynamic Symposium. *Stroke* 26, 1123. 1995.

[17] C. J. McMahon, P. McDermott, D. Horsfall, J. R. Selvarajah and King. The reproducibility of transcranial Doppler middle cerebral artery velocity measurements: implications for clinical practice. *British Journal of Neurosurgery* 21, 21--7. 2007.

[18] B. Giannone. BG-Rescue Linux. . 2010. *http://www.giannone.ch/rescue/current/*.

[19] Various. PyQt. Riverbank Computing Limited. 2011. *http://www.riverbankcomputing.co.uk/software/pyqt/*.

[20] J. Sanders. Veusz - A Scientific Plotting Package. . 2010. *http://home.gna.org/veusz/*.

[21] M. Farhoudi, S. Kermani and H. Sadeghi-Bazargani. Relatively higher norms of blood flow velocity of major intracranial arteries in North-West Iran. *BMC research notes* 3, 174. 2010.

[22] S. Tang, J. Jeng, P. Yip, C. Lu, B. Hwang, W. Lin and H. Liu. Transcranial color-coded sonography for the detection of middle cerebral artery stenosis.. *Journal of Ultrasound in Medicine* 24, 451--7; quiz 459--60. 2005.

[23] P. A. P. Jesus, R. M. Vieira-de-Melo, F. J. F. B. Reis, L. C. Viana, A. Lacerda, J. S. Dias and J. Oliveira-Filho. Cognitive dysfunction in congestive heart failure: transcranial Doppler evidence of microembolic etiology. *Arquivos de Neuro-Psiquiatria* 64, 207--210. 2006.

[24] J. A. Zagzebski. *Essentials of Ultrasound Physics*. : Mosby. 1996.